

**ELECTROFABRICATION OF ZINC OXIDE
PHOTOCATALYST IN THE PRESENCE OF
BIO-WASTE EXTRACTS AND DEEP EUTECTIC
SOLVENT FOR DEGRADATION OF
2,4-DICHLOROPHENOL**

AUNIE AFIFAH BINTI ABDUL MUTALIB

UNIVERSITI SAINS MALAYSIA

2025

**ELECTROFABRICATION OF ZINC OXIDE
PHOTOCATALYST IN THE PRESENCE OF
BIO-WASTE EXTRACTS AND DEEP EUTECTIC
SOLVENT FOR DEGRADATION OF
2,4-DICHLOROPHENOL**

by

AUNIE AFIFAH BINTI ABDUL MUTALIB

**Thesis submitted in fulfillment of the requirements
for the degree of
Doctor of Philosophy**

July 2025

ACKNOWLEDGEMENT

First and foremost, I extend my heartfelt gratitude to my esteemed supervisor, Dr. Nur Farhana Jaafar, for her invaluable guidance and unwavering support throughout this journey. Her scholarly insights and mentorship have been a beacon of inspiration, shaping the trajectory of my research and facilitating the realization of this academic achievement. I am equally thankful to my co-supervisors, Dr. Mazidatulakmam Miskam and Dr. Thanchanok Ratvijitvech, for their vital contributions, providing essential materials and offering thoughtful advice that enriched my work. Acknowledgment is also due to my dedicated lab mate, Tasnim Aisyah Binti Mahmulee Torlaema, whose selfless collaboration and unwavering support have played a pivotal role in advancing this study. My PhD journey would not have been possible without the financial assistance provided by the Excellent Student Program granted by Jabatan Perkhidmatan Awam (JPA).

To my family, especially my beloved mother, Wan Zalmiah Wan Zakaria, I owe immense gratitude for her unwavering faith, and boundless love, which have been steadfast sources of strength throughout this endeavor.

Lastly, and most importantly, I am profoundly indebted to the cherished memory of my late father, Abdul Mutalib Abdullah, whose unwavering belief in my potential continues to inspire and propel me forward. Though absent, his enduring legacy remains a guiding light in my life and this academic pursuit.

TABLE OF CONTENTS

ACKNOWLEDGEMENT	ii
TABLE OF CONTENTS	iii
LIST OF TABLES	vii
LIST OF FIGURES	viii
LIST OF SYMBOLS	xii
LIST OF ABBREVIATIONS	xiv
LIST OF APPENDICES	xvi
ABSTRAK	xvii
ABSTRACT	xix
CHAPTER 1 INTRODUCTION	1
1.1 Research Background.....	1
1.2 Problem Statement	4
1.3 Objectives.....	5
1.4 Scope of Study	6
1.5 Significance of Study	8
1.6 Thesis Outline	10
CHAPTER 2 LITERATURE REVIEW	12
2.1 Chlorophenol Derivatives as an Emerging Organic Pollutant	12
2.1.1 Properties and Sources	12
2.1.2 Exocological and Human Impacts.....	14
2.1.3 The Removal Technology	16
2.2 Types of AOP Mechanism for Pollutant Degradation	19
2.3 ZnO Semiconductor Photocatalyst.....	20
2.3.1 Properties of ZnO	21
2.3.2 General Mechanism of ZnO in Pollutant Degradation.....	23

2.3.3	Factors that Impact ZnO Performance	25
2.4	Common ZnO Synthesis Routes	32
2.4.1	Sol-Gel	32
2.4.2	Hydrothermal	33
2.4.3	Co-Precipitation	34
2.4.4	Microwave Method	35
2.5	Electrochemical Synthesis of ZnO Photocatalyst	35
2.5.1	Components and Principles of Electrochemical Synthesis	36
2.5.2	Influence of Electrolyte in Photocatalyst Electrochemical Synthesis.....	42
2.6	Potential of Plant Extract for More Sustainable ZnO Electrosynthesis	44
2.7	Deep Eutectic Solvent (DES).....	48
2.7.1	Properties of DES.....	49
2.7.2	Green aspect of DES	52
2.7.3	Potential of DES as Supporting Electrolyte.....	55
2.8	Summary	58
CHAPTER 3 METHODOLOGY.....		59
3.1	Introduction	59
3.2	Materials.....	61
3.3	Plant Extract Preparation Method	62
3.4	Phytochemical Assays.....	64
3.4.1	Total Phenolic Assay.....	64
3.4.2	Total Flavanoid Assay.....	64
3.4.3	Total Reducing Power Assay	65
3.5	Deep Eutectic Solvent Synthesis.....	65
3.6	Conductivity Measurement of Electrolyte	66
3.7	Electrochemical Synthesis of ZnO	66
3.8	Characterization of ZnO	67

3.8.1	Crystallographic Analysis	67
3.8.2	Surface Functional Group Analysis	69
3.8.3	Optical Band Gap Measurement	70
3.8.4	Particle Size Distribution Analysis	70
3.8.5	Surface Morphology Characterization	71
3.8.6	Textural Properties Measurement	71
3.8.7	Elemental and Chemical States Analysis	72
3.8.8	Particle Structure Analysis	72
3.9	Photocatalytic Degradation	73
3.10	Scavenger Studies	74
3.11	Reusability Studies	75
3.12	GC-MS Analysis for Degradation Mechanism Determination	75
CHAPTER 4 RESULT AND DISCUSSION.....		77
4.1	Effects of Different Plant Extracts and the Extraction Method	77
4.1.1	Phytochemical Analysis of the Plant Extracts.....	77
4.1.2	Effect on ZnO Physicochemical Properties	100
4.1.3	Proposed Mechanism of Bio-mediated ZnO Formation	98
4.1.4	Effect on Photocatalytic Performance.....	100
4.2	Effects of DES Incorporation as Supporting Electrolyte	103
4.2.1	Effect on Electrolyte Conductivity.....	104
4.2.2	Effect on ZnO Physicochemical Properties	105
4.2.3	Proposed Formation Mechanism.....	122
4.2.4	Effect on Photocatalytic Activity	125
4.3	The 2,4-DCP Degradation Evaluations	128
4.3.1	Optimum Reaction Parameters	128
4.3.2	Kinetic Analysis	132
4.3.3	Scavenger Studies	135

4.3.4	Reusability Analysis.....	137
4.4	The Degradation Pathway of 2,4-DCP.....	138
4.5	Photocatalytic Performance on Other Pollutants	143
4.6	Comparison with the Previous Studies.....	144
CHAPTER 5 CONCLUSION AND FUTURE RECOMMENDATIONS....		147
5.1	Conclusion.....	147
5.2	Recommendations for Future Research	149
REFERENCES.....		151
APPENDICES		
LIST OF PUBLICATIONS		
LIST OF AWARDS		
LIST OF CONFERENCES		

LIST OF TABLES

	Page
Table 2.1	The ZnO basic physical parameters23
Table 2.2	Summarization of aspects that impact the photocatalytic activity of ZnO31
Table 2.3	The general electrochemical behavior of DES-based electrolytes in previous literature.....56
Table 3.1	The list of chemicals used in this study62
Table 4.1	The phytochemical analysis of the prepared extract in this study78
Table 4.2	The structural analysis and Rietveld fit parameters of the synthesized ZnO.....85
Table 4.3	The band gap of ZnO catalysts in this study88
Table 4.4	Overall surface measurement analysis of the synthesized ZnO.....93
Table 4.5	The productivity of the electrolyte mixture in this work105
Table 4.6	The structural analysis and Rietveld fit parameters of the synthesized ZnO.....115
Table 4.7	The BET surface area, and pore size measurement of the synthesized ZnO.....120
Table 4.8	The kinetic analysis of 2,4-DCP degradation by ZnO-1.0 at different concentrations.....134
Table 4.9	The comparison of the 2,4-DCP degradation efficiencies by ZnO-1.0 synthesized in this work with other reported ZnO from the previous literature.....146

LIST OF FIGURES

	Page
Figure 2.1	Chemical structures of the most common commercial chlorophenols: (1) 2,4-dichlorophenol (2,4-DCP), (2) pentachlorophenol (PCP), (3) 2,4,5-trichlorophenol (2,4,5-TCP), (4); 2-chlorophenol (2-CP) and (5) 4-chlorophenol (4-CP)..... 13
Figure 2.2	The illustrated ZnO's wurtzite structure (Sharma et al., 2022).....22
Figure 2.3	The photocatalytic mechanism by ZnO24
Figure 2.4	The general sol-gel synthesis route (Zahra et al., 2022).33
Figure 2.5	The schematic illustration of the autoclave system for the hydrothermal method (Ganguly et al., 2019).....34
Figure 2.6	The mediated (a) and non-mediated (b) electrosynthesis of ZnO via anodic dissolution method38
Figure 2.7	The properties of anodized TiO ₂ nanotubes.....39
Figure 2.8	The metal nanoparticle synthesis in the presence of plant extract (Kamarudin et al., 2021)46
Figure 2.9	The example of HBAs and HBDs for the synthesis of DES (Smith et al., 2014).....49
Figure 3.1	The flowchart of the overall research flow61
Figure 3.2	The general plant extract strategies employed in this study63
Figure 3.3	The schematic illustration of the electrosynthesis setup used in this study67
Figure 3.4	The schematic illustration of the phoreactor used in this study 73
Figure 4.1	The FTIR analysis of the calcined ZnO: (a) commercial ZnO, (b) ZnO-TLR (c) ZnO-BP, (d) ZnO-SCG (e) ZnO-SCG-MW (f) ZnO-SCG-UAE81

Figure 4.2	The XRD patterns of the synthesized ZnO commercial, ZnO-SCG, ZnO-TLR, ZnO-BP, ZnO-SCG-MW, and ZnO-SCG-UAE	82
Figure 4.3	The refined XRD pattern of ZnO commercial, ZnO-SCG, ZnO-TLR and ZnO-BP, ZnO-SCG-MW, and ZnO-SCG-UAE using the Rietveld mode	84
Figure 4.4	The UV-Vis-DRS reflectance data of ZnO commercial, ZnO-SCG, ZnO-TLR, ZnO-BP, ZnO-SCG-MW and ZnO-SCG-UAE	87
Figure 4.5	The band gap of the ZnO commercial, ZnO-TLR and ZnO-BP (A) and ZnO-SCG-UAE, ZnO-SCG-MW and ZnO-SCG (B)	89
Figure 4.6	The particle size distribution of ZnO commercial, ZnO-SCG, ZnO-TLR, ZnO-BP, ZnO-SCG-MW and ZnO-SCG-UAE.....	90
Figure 4.7	The TEM analysis of the ZnO commercial, ZnO-SCG, ZnO-TLR, ZnO-BP, ZnO-SCG-MW and ZnO-SCG-UAE	92
Figure 4.8	The (A) adsorption-desorption isotherm plots and (B) BJH pore distribution plot of ZnO commercial, ZnO-SCG, ZnO-TLR, ZnO-BP, ZnO-SCG-MW and ZnO-SCG-UAE.....	94
Figure 4.9	The Zn 2p spectra XPS spectral of ZnO commercial, ZnO-SCG, ZnO-BP, ZnO-TLR, ZnO-SCG-MW, and ZnO-SCG-UAE	95
Figure 4.10	The deconvoluted O 1s spectral of ZnO using Gaussian-Lorentzian fit (A-E), and (G) the intensity of each peak (based on peak area)....	97
Figure 4.11	The FTIR (A) and XRD (B) analysis of the ZnO-SCG sample before and after calcination.....	98
Figure 4.12	The possible formation mechanism of the SCG extract-assisted electrosynthesized ZnO in this study.	100
Figure 4.13	Photocatalytic degradation of 2,4-DCP (30 mg L ⁻¹) using (A) ZnO-commercial, ZnO-TLR, and ZnO-BP, and (B) ZnO-SCG, ZnO-SCG-MW, and ZnO-SCG-UAE under fixed conditions (0.019 g catalyst, pH 3, 480 min).	103
Figure 4.14	The FTIR spectral of ZnO-0.1, ZnO-0.5 and ZnO-1.0 samples	106

Figure 4.15	(A) The Zn 2p XPS spectral, (B) deconvoluted Zn 2p _{3/2} spectra, (C) deconvoluted C1s spectra, and (D) deconvoluted O 1s spectral of ZnO-DES samples.	108
Figure 4.16	The XRD pattern of ZnO-0.1, ZnO-0.5 and ZnO-1.0.....	110
Figure 4.17	The Rietveld refinements of the ZnO-0.1, ZnO-0.5 and ZnO-1.0...	111
Figure 4.18	The generated cell unit image from the Rietveld output using Vesta software (the minor white line on the oxygen atom indicated the unoccupied sites) of the ZnO photocatalyst.	113
Figure 4.19	The SEM images of the ZnO-0.1, ZnO-0.5 and ZnO-1.0.....	116
Figure 4.20	The TEM images of the ZnO-0.1, ZnO-0.5 and ZnO-1.0 catalyst of 20 k magnification and 50 k magnification.	116
Figure 4.21	The particle size distribution of ZnO-0.1, ZnO-0.5 and ZnO-1.0....	118
Figure 4.22	(A) The N ₂ adsorption-desorption isotherms and (B) the BJH pore distribution plot of the synthesized ZnO photocatalysts.....	120
Figure 4.23	(A) The reflectance measurement from diffuse reflectance spectroscopy and derived Kubelka-Munk function versus energy plot (B) of the synthesized ZnO.....	122
Figure 4.24	The FTIR analysis of the ZnO-1.0 sample before and after the calcination process	124
Figure 4.25	The possible formation mechanism of ZnO in this study	125
Figure 4.26	The degradation percentage vs time plot of 2,4-DCP pollutants in the presence of the electrosynthesized ZnO in the reaction conditions of 0.019 g catalyst, pH 3, 30 mg L ⁻¹ pollutant, and 420 min reaction.....	126
Figure 4.27	The effect of pH on the photocatalytic activity of ZnO-1.0 (Reaction conditions: 420 min reaction, 0.019 g catalyst, and 10 mg L ⁻¹ 2,4-DCP	129
Figure 4.28	The effect of catalyst loading on the photocatalytic activity of ZnO-1.0 (Reaction conditions: 420 min reaction, 10 mg L ⁻¹ and pH 3 2,4-DCP.....	130

Figure 4.29	The effect of initial pollutant concentration on the photocatalytic activity of ZnO-1.0 (Reaction conditions: 420 min reaction, 0.019 g catalyst loading and pH 3 2,4-DCP).....	131
Figure 4.30	The $\ln (C_0/C_t)$ plot against time (min).....	133
Figure 4.31	Plot $1/r_0$ against $1/C_0$	134
Figure 4.32	The photodegradation performance of ZnO-1.0 in the presence of scavengers (Reaction conditions: 30 mg L ⁻¹ , pH 3 pollutant, 0.019 g catalyst and 420 min).....	137
Figure 4.33	The photodegradation performance of ZnO-1.0 at repeated cycles.	138
Figure 4.34	The GC-MS analysis of the collected water sample at respective reaction times (initial, after 2,3, and 5 hours).	141
Figure 4.35	The proposed degradation pathway of 2,4-DCP in this study	142
Figure 4.36	The degradation percentages of other pollutants using ZnO-1.0 (Reaction conditions: 0.019 g catalyst, pH 3, 30 mg L ⁻¹ , and 420 min).	144

LIST OF SYMBOLS

%	Percentage
μS	Micro siemens
$\cdot\text{OH}$	Hydroxyl radicals
$^{\circ}\text{C}$	Degree Celsius
χ^2	Reduced chi-square
\AA	Ampere
C_0	Initial concentration
cm	Centimetre
C_t	Concentration at time,t
e^-	Electron
e^-_{cb}	Electron in the conduction band
E_g	Band gap
eV	Electron volt
g	Gram
g L^{-1}	Gram per litre
h	Planck constant
h^+	Positive electron
h^+_{vb}	Positive electron at the valence band
K	Kelvin
k	Shape factor
k_{app}	Apparent first order rate constant
kg	Kilogram
K_{LH}	Adsorption coefficient of the reactant
k_r	Reaction rate constant

kV	Kilo volt
mA	Milli Ampere
mg	Milligram
mg L ⁻¹	Milligram per liter
min	Minute
mL	Mililitre
nm	nanometer
pH _{pzc}	Point of zero charge
R _p	Residual error
R _{wp}	Weighted residual error
V	Volt
W	Watt
δ	Dislocation density
θ	Theta
A _a	Total area of amorphous phase
A _c	The total area of the crystalline phase
D	Crystalline size
X _c	Crystallinity percentage
β	Full width at half maximum
λ	Lambda

LIST OF ABBREVIATIONS

2,4-DCP	2,4-Dichlorophenol
AOP	Advanced oxidation process
BET	Bruanacur- Emmet-Teller
BP	Banana peel
CP	Chlorophenol
DCM	Dichloromethane
DES	Deep eutectic solvent
DMF	Dimethylformamide
SEM	Field Emission Scanning Electron Microscopy
FTIR	Fourier Transform Infrared Spectroscopy
FWHM	Full width at half maximum
GC-MS	Gas chromatography-mass spectrometry
HRTEM	High-Resolution Transmission Electron Microscopy
IL	Ionic liquid
IUPAC	International Union of Pure and Applied Chemistry
L-H	Langmuir-Hinshelwood
MW	Microwave
SCG	Spent coffee ground
SDG	Sustainable development goals
TC	Texture coefficient
THF	Tetrahydrofuran
TEM	Transmittance Electron Microscopy
TLR	Tea leaves residue
UAE	Ultrasonic-assisted extraction

UN	United Nations
USM	Universiti Sains Malaysia
UV	Ultraviolet
UV-Vis	Ultraviolet-visible
UV-Vis-DRS	UV-Vis Diffuse Reflectance Spectroscopy
XPS	X-ray Photoelectron Spectroscopy
XRD	X-ray Diffraction

LIST OF APPENDICES

Appendix A	Standard calibration of catechin hydrate
Appendix B	Standard calibration of ascorbic acid
Appendix C	Standard calibration of gallic acid
Appendix D	Color changes observation during phytochemical assay
Appendix E	Standard calibration of 2,4- DCP at pH 3
Appendix F	Standard calibration of 2,4-DCP at pH 5
Appendix G	Standard calibration of 2,4-DCP at pH 7
Appendix H	Standard calibration of 2,4-DCP at pH 9
Appendix I	Standard calibration of 2,4-DCP at pH 11
Appendix J	Examples of the UV-Vis spectra of 2,4-DCP degradation at pH 3
Appendix K	GC-MS instrument settings for degradation compound detection

**ELEKTROFABRIKASI FOTOKATALIS ZINK OKSIDA DENGAN
KEHADIRAN SISA-BIO EKSTRAK DAN PELARUT EUTEKTIK DALAM
UNTUK PENGURAIAN 2,4-DIKLOROFENOL**

ABSTRAK

Klorofenol seperti 2,4-diklorofenol (2,4-DCP) merupakan bahan pencemar berbahaya yang lazim ditemui dalam air sisa industri, yang memerlukan pembangunan kaedah fotokatalitik hijau dan berkesan untuk penghapusannya. Kajian ini mencadangkan elektrosintesis ZnO yang lestari menggunakan ekstrak bio-sisa dan pelarut eutektik dalam (DES) sebagai elektrolit hijau. Bio-sisa seperti sisa kopi terpakai (SCG), sisa daun teh (TLR), dan kulit pisang (BP) diterokai sebagai alternatif elektrolit mesra alam kerana ketersediaannya yang meluas serta kandungan antioksidan semula jadi yang tinggi, termasuk flavonoid dan fenolik. Kaedah pengekstrakan berasaskan air secara mudah telah dipilih kerana kesenangan operasi dan kesesuaiannya untuk penskalaan. Untuk perbandingan, kaedah pengekstrakan bantuan gelombang mikro (MW) dan bantuan ultrasonik (UAE) turut digunakan kerana ia diketahui berkesan dalam meningkatkan perolehan sebatian bioaktif dan hasil antioksidan. Ujian fitokimia seperti kuasa pereduksi, jumlah fenolik dan kandungan flavonoid dijalankan untuk mengesahkan dan menganggarkan kandungan fitokimia ekstrak tersebut. Katalis ZnO yang dihasilkan secara elektrosintesis hijau kemudiannya dicirikan menggunakan FTIR, SEM, PSA, BET, TEM, UV-Vis DRS, XRD, dan XPS. Antara ekstrak-ekstrak tersebut, SCG yang disediakan melalui pengekstrakan air mudah menghasilkan kandungan flavonoid dan kuasa pereduksi tertinggi, sekaligus menghasilkan ZnO-SCG dengan kehabluran yang ditambah baik, peningkatan kekosongan oksigen permukaan, saiz zarah yang lebih kecil, serta jalur

tenaga yang berkurangan. ZnO-SCG mencapai penguraian 92.6 % bagi 30 mg L⁻¹ 2,4-DCP pada pH 3 dengan penggunaan katalis 0.019 g dalam masa 480 minit. Pada bahagian kedua kajian, pelarut eutektik dalam (DES) yang disintesis daripada klorida kolina (ChCl) dan klorida zink (ZnCl₂) digunakan sebagai elektrolit sokongan untuk meningkatkan sintesis ZnO, berikutan sifatnya yang boleh terbiodegradasi, kadar toksik rendah dan kemampuannya mengawal pertumbuhan kristal serta morfologi zarah. Jumlah berbeza (0.1, 0.5, dan 1.0 mL) ditambah ke dalam ekstrak SCG, menghasilkan ZnO-0.1, ZnO-0.5, dan ZnO-1.0. Kekonduksian meningkat dengan pertambahan isipadu DES, mencapai $5.06 \times 10^4 \mu\text{S cm}^{-1}$. ZnO-1.0 menunjukkan ciri-ciri yang dipertingkatkan seperti saiz hablur yang lebih besar (57.0 nm), zarah berbentuk rod yang lebih kecil (145 μm), dan kadar kekosongan oksigen yang tinggi (55.5 %), membolehkan penghapusan 94.8 % 2,4-DCP dalam masa 420 minit di bawah cahaya tampak. Ujian fotodegradasi mengesahkan keadaan optimum pada penggunaan 0.019 g ZnO-1.0, pH 3, dan kepekatan pencemar 30 mg L⁻¹. ZnO-1.0 mengekalkan kecekapan sebanyak 80 % selepas tiga kitaran, dengan kinetik tindak balas mengikuti model pseudo-order pertama dan lubang fotogenerasi dikenalpasti sebagai spesies reaktif utama. Analisis GC-MS mengesan hasil sampingan mineralisasi seperti fenol, asid benzoik, dan quinon, sekali gus menunjukkan potensi fotokatalis ZnO-1.0 yang disintesis secara hijau dalam penguraian berkesan bahan cemar organik.

**ELECTROFABRICATION OF ZINC OXIDE PHOTOCATALYST IN THE
PRESENCE OF BIO-WASTE EXTRACTS AND DEEP EUTECTIC
SOLVENT FOR DEGRADATION OF 2,4-DICHLOROPHENOL**

ABSTRACT

Chlorophenols such as 2,4-dichlorophenol (2,4-DCP) are common hazardous pollutants found in industrial wastewater, necessitating the development of green and effective photocatalytic methods for their removal. This study proposes a sustainable ZnO electrosynthesis using bio-waste extracts and deep eutectic solvent (DES) as a green electrolyte. The bio-wastes, including spent coffee grounds (SCG), tea leaf residues (TLR), and banana peel (BP), were explored as an alternative eco-friendly electrolyte due to their abundance and high content of natural antioxidants, such as flavonoids and phenolics. A facile water-based extraction method was primarily selected due to its operational simplicity and suitability for scale-up. For comparison, microwave-assisted (MW) and ultrasonic-assisted extraction (UAE) methods were also included, as they are known for their efficiency in enhancing the recovery of bioactive compounds and improving antioxidant yield. The phytochemical assays, including reducing power, total phenolic, and flavonoid content, were conducted to confirm and estimate the phytochemical constituents of the extracts. The green electrosynthesized ZnO catalysts were then characterized via FTIR, SEM, PSA, BET, TEM, UV-Vis DRS, XRD, and XPS. Among the extracts, SCG prepared via facile water extraction yielded the highest flavonoid content and reducing power, resulting in ZnO-SCG with improved crystallinity, enhanced oxygen vacancies, smaller particle size, and a reduced band gap. ZnO-SCG achieved 92.6 % degradation of 30 mg L⁻¹ 2,4-DCP at pH 3 using 0.019 g catalyst in 480 min. In the second part of the study, a

deep eutectic solvent (DES) synthesized from choline chloride (ChCl) and zinc chloride (ZnCl_2) was incorporated as a supporting electrolyte to enhance ZnO synthesis, owing to its biodegradable, low-toxicity characteristics and its ability to direct crystal growth and morphology. Different volumes (0.1, 0.5, and 1.0 mL) were added to the SCG extract, producing ZnO-0.1, ZnO-0.5, and ZnO-1.0. Conductivity increased with DES volume, reaching $5.06 \times 10^4 \mu\text{S cm}^{-1}$. ZnO-1.0 exhibited improved features such as larger crystallite size (57.0 nm), smaller rod-like particles (145 μm), and high oxygen vacancies (55.5 %), enabling 94.8 % 2,4-DCP removal within 420 min under visible light. Photodegradation tests confirmed optimal conditions at 0.019 g ZnO-1.0, pH 3, and 30 mg L^{-1} pollutant. ZnO-1.0 maintained 80 % efficiency over three cycles, with pseudo-first-order kinetics and photogenerated holes as the dominant reactive species. GC-MS analysis revealed mineralization by-products, including phenol, benzoic acid, and quinone, highlighting the potential of the green-synthesized ZnO-1.0 photocatalyst for effective organic contaminant degradation.

CHAPTER 1

INTRODUCTION

1.1 Research Background

Water and sanitation aspects are specifically addressed in the Sustainable Development Goals (SDG (6)) agenda, with the goal of "ensuring the availability and sustainability of water and sanitation for all." Unfortunately, based on current trends, it is reported that more than half of the earth's population will suffer water scarcity at least once a month by 2050 (Boretti & Rosa, 2019). Water contamination is one of the identified reasons for this salient issue. While water demand soars in tandem with global population growth, pollution deprives clean water resources (Dihom et al., 2022). According to statistics, the annual disposal of sewage and other effluents is 730 million tonnes. Meanwhile, industrial discharge emits at least 300 megatons of wastewater annually, with over 80 % of the total being unattended (Boretti & Rosa, 2019). Parallel with the current rate of growing contaminant lists (persistent organic pollutants (POPs), inorganic materials, macroscopic pollutants, etc.), water pollution will skyrocket, adversely affecting not only sustainable development but also global well-being in general.

The necessity for water treatment or reclamation becomes increasingly pressing. Various water treatment technologies have been expanded for this goal, but high costs typically hamper their implementation (Ong et al., 2018; Plakas & Karabelas, 2012). Nevertheless, a substantial number of researchers are interested in the semi-conductive photocatalysis technology, which is known for its economic benefits as well as being a simple, eco-friendly, and viable way (Low et al., 2017).

Many photocatalyst fabrication routes have been established to produce photocatalysts with high photo-reactivity. Electrochemical, sol-gel, hydrothermal, solvothermal, ultrasonic-assisted, and wet-impregnation methods are some of the examples. The electrochemical method, as a liquid-phase chemical technique incorporating electrons supplied by an external circuit, is well known for its adaptability in designing photocatalyst structures (Bahnemann et al., 2022). Furthermore, this technique provides a mechanistic path and has a high potential for scalability, which is critical when considering mass or industrial-scale catalyst production (Wang et al., 2018).

In the electrochemical method, the electrolyte system plays a major part in determining the efficiency of the fabrication process. Aprotic organic solvents such as dimethylformamide (DMF), tetrahydrofuran (THF), and acetone nitrile have been widely used as the electrolytic medium to dissolve the salt components or additives (Khairol & Sapawe, 2018). However, when considering large-scale photocatalyst production, the involvement of these organic-based chemicals can impact the environment negatively. Therefore, many researchers are now adapting the green electro-fabrication routes by exploiting the antioxidant components of the plant extract commonly, phenolic compounds to act as reducing agents (Khairul Hanif Mohd Nazri & Sapawe, 2020; Khandel et al., 2018; Küünal et al., 2018). For example, Sapawe et al. tested on malachite green (MG) degradation resulting 91.7 %, 94.0 %, 98.5 %, and 97.3 % by implementing AgO, CuO, ZnO, and NiO catalysts synthesized in crude plant extract respectively (Sapawe et al., 2019). Even though many types of raw plant extracts can be employed to benefit photocatalyst synthesis due to the common phenolic content, the plant waste materials should be preferred first to reduce the cost of raw resources exploitation. Moreover, a substantial number of studies have proved that the bioactive

component in plant waste such as banana peels (BP), tea leaves residue (TLR), and spent coffee grounds (SCG) can be extracted by just simple and straightforward water-based extraction routes (Bankar et al., 2010; Geetha, 2015; Ibrahim, 2015; Peel et al., 2022; Sriarumtias & Najihudin, n.d.; Tyagi et al., 2021).

Previously, there was an attempt to integrate the reducing properties of the plant extract with the ionic liquid (IL). The research found that the synergistic effect between the supramolecular properties and templating behavior of ILs can help in generating smaller particles and a larger surface area of the resultant photocatalyst (Kamarudin et al., 2021). However, several works of literature have criticized the overuse green label associated with IL since the IL preparation involves high cost and very complicated procedures, contradicting their stipulated properties e.g., sustainable and eco-friendly (Abo-hamad et al., 2015; Chen & Mu, 2021; Płotka-Wasyłka et al., 2020; Tahir et al., 2021). Therefore, the eutectic mixture of hydrogen bond donor and hydrogen acceptor in a certain ratio (commonly 1:1 to 1:2), known as deep eutectic solvent (DES) is regarded as the potential alternative to ILs due to its almost similar templating ability, despite being much less cost, and more straightforward preparation procedures (Smith et al., 2014; Yang, 2019; M. Zhang et al., 2021).

Therefore, this research explores the synergistic effect of combined low-cost SCG extract with DES as a single electrolyte system and its impact on the structure and functionality of electro-fabricated ZnO. Before the DES incorporation into the plant extract, the effect of plant extract variations, the influence of the extraction procedures, and the phytochemical content on the structural and chemical properties of ZnO were studied. Subsequently, the electrolyte was further developed by incorporating different volumes of DES, which were then evaluated based on the photocatalytic performance

of the resulting ZnO. The photoactivity of synthesized ZnO were tested with 2,4-dichlorophenol (2,4-DCP) under various parameters. In the presence of the best catalyst, the optimization of the reaction conditions was performed along with the kinetic, Scavenger, and reusability studies. Lastly, the detailed mechanistic pathway of the 2,4-DCP compound was then proposed using the GC-MS analysis.

1.2 Problem Statement

The global scarcity of clean water continues to worsen due to rising demand and increasing pollution from industrial, agricultural, and municipal sources. Persistent pollutants such as chlorinated phenols, dyes, and pharmaceutical residues pose serious threats to human health and environmental stability. Although various water treatment technologies exist, many require high energy input, generate secondary waste, and involve costly upkeep, making them less viable for long-term use, particularly in developing regions. Consequently, interest has shifted toward sustainable alternatives like semiconductor-based photocatalysis, which uses light energy to break down organic contaminants without additional chemicals.

Despite its potential, the large-scale adoption of photocatalytic systems remains limited by challenges in material synthesis. Conventional fabrication methods often rely on toxic organic solvents like DMF and acetonitrile, which, while effective, undermine sustainability by introducing environmental hazards. As demand for scalable photocatalyst production rises, there is a growing need for synthesis methods that align with green chemistry principles.

One such approach involves using plant-based extracts as natural reducing agents. Agricultural wastes like BP, TLR, and SCG are rich in polyphenols and

bioactive compounds that support nanoparticle formation. This not only enables greener synthesis but also helps address biomass waste. However, improvements in reaction control, particle consistency, and photocatalytic performance are still necessary to meet real-world application standards.

In addition to bio-based materials, DES, formed from biodegradable components, also serves as an alternative to conventional solvents. Their low toxicity, simple synthesis, and structure-directing properties enable control over nucleation, growth, and surface features of nanomaterials, making them compatible with plant-derived reducing agents.

Yet, the integration of DES and plant waste extracts in electrochemical synthesis remains insufficiently explored. Given their complementary properties, this study hypothesized that combining DES with plant-derived extracts could enhance the electrochemical synthesis of photocatalysts and improve ZnO performance while promoting a more sustainable and eco-friendly production route.

1.3 Objectives

The objectives of this study are:

1. To study the effect of plant extract, extraction methods, and DES volume on the electrosynthesis of ZnO photocatalysts.
2. To examine the physicochemical properties of the electrosynthesized ZnO photocatalysts.
3. To evaluate the photoactivity of the ZnO on the degradation of 2,4-DCP
4. To scrutinize the kinetics and propose the mechanism of the photodegradation of 2,4-DCP over ZnO.

1.4 Scope of Study

This study encompasses four main parts, which are:

1. The study of the effect of plant extract, extraction methods, and DES volume on the electrosynthesis of ZnO photocatalysts.

The first part of the study focuses on the preparation of green electrolytes using three different waste plant sources: SCG, TLR, and BP. These extracts were obtained through three different methods: facile water-based extraction, microwave-assisted extraction (MW), and ultrasonic-assisted extraction (UAE). Phytochemical assessments, including reducing power, total phenolic content, and flavonoid content, were carried out to estimate the concentration of bioactive compounds in each extract.

Following extract preparation, ZnO was synthesized electrochemically using each variant, and the resulting photocatalysts were screened for their photodegradation performance toward 2,4-DCP. Based on this evaluation, the most effective plant source and extraction method were identified for further optimization. Subsequently, DES, specifically 0.1 mL, 0.5 mL, and 1.0 mL, was incorporated into the selected plant extract as a supporting electrolyte. Electrolyte conductivity and ZnO yield were measured to evaluate the influence of DES volume. The physicochemical and photocatalytic effects of DES incorporation were further examined, and the role of DES in ZnO formation was inferred.

2. The examination of the physicochemical properties of the electrosynthesized ZnO photocatalysts.

A range of characterization techniques was employed to evaluate the physicochemical properties of the synthesized ZnO photocatalysts. Fourier-transform infrared spectroscopy (FTIR) was used to identify functional groups, while scanning electron microscopy (SEM) and transmission electron microscopy (TEM) analyzed surface morphology and particle structure. Particle size analysis (PSA) determined size distribution, and X-ray diffraction (XRD) examined crystallinity. X-ray photoelectron spectroscopy (XPS) provided information on surface elemental composition and chemical states. The nitrogen adsorption-desorption isotherms method assessed surface area and porosity, while UV-Vis diffuse reflectance spectroscopy (UV-Vis DRS) measured optical properties and band gap. These analyses were used to compare the effects of plant extract types, extraction methods, and DES volumes, and to support the proposed formation mechanism of bio-mediated electrosynthesized ZnO.

3. The evaluation of the photoactivity of the ZnO on the degradation of 2,4-DCP.

The third part of the study involves evaluating the photocatalytic performance of the optimized ZnO photocatalyst in degrading 2,4-DCP under UV light. Several operational parameters were varied, including initial solution pH (ranging from 3 to 11), catalyst dosage ($0.01\text{--}0.049\text{ g L}^{-1}$), and initial pollutant concentration ($10\text{--}100\text{ mg L}^{-1}$), to assess their impact on degradation efficiency. The catalyst's reusability was also tested over multiple cycles to examine its stability and operational feasibility in repeated applications.

4. The kinetics behavior and the mechanism of the photodegradation of 2,4-DCP over ZnO.

To gain insight into the degradation mechanism, kinetic analysis was performed using the Langmuir-Hinshelwood model, which enabled a better understanding of the reaction behavior at the solid-liquid interface. Scavenger studies were conducted using specific scavengers, sodium oxalate (h^+), potassium iodide (e^-), and potassium peroxydisulfate ($\cdot\text{OH}$) to identify the predominant reactive species involved in the photocatalytic process. Furthermore, gas chromatography-mass spectrometry (GC-MS) analysis was employed to monitor the intermediate products formed at different reaction intervals (0 h, 2 h, 3 h, and 5 h). Based on these results, a plausible degradation pathway for 2,4-DCP leading to final mineralized products was proposed.

1.5 Significance of Study

This study addresses an urgent concern in sustainable wastewater treatment by introducing an environmentally conscious and cost-efficient method for photocatalyst production. The growing presence of pollutants in water systems threatens both ecological balance and public health, demanding solutions that are both effective and sustainable. Among available technologies, semiconductor photocatalysis offers a clear advantage due to its ability to break down pollutants into harmless by-products, rather than merely transferring them to another phase. Despite its promise, the practical application of this method remains limited by the high cost of catalyst synthesis and the frequent use of toxic solvents, factors that run counter to the principles of green chemistry.

To help overcome these challenges, this research explored a new synthesis pathway for ZnO photocatalysts by utilizing waste materials, specifically plant-derived extracts, and combining them with DES in a green electrochemical fabrication process. This approach supports resource reuse while reducing dependency on harmful chemicals. The choice of plant waste, such as spent coffee grounds, helps lower production costs and promotes sustainable material sourcing. DES, serving as a more environmentally sound alternative to conventional organic solvents, further enhances the green value of the synthesis route.

This study emphasized the detailed comparison of different plant types, extraction methods, and DES volumes to understand their effects on the properties and performance of the resulting ZnO. Through this process, a ZnO photocatalyst was developed with improved structural features and photocatalytic activity, particularly in degrading 2,4-DCP as a model organic pollutant. The research also provides insight into the reaction mechanism by analyzing degradation pathways and tracking intermediate products using GC-MS. Complementary kinetic studies and scavenger experiments support a clearer understanding of how the catalyst works during photodegradation.

In summary, this work presents a green and practical route for producing photocatalysts that can support cleaner wastewater treatment practices. By combining waste-based resources with environmentally safer solvents, the study not only reduces the impacts of synthesis but also enhances the effectiveness of pollutant breakdown. These contributions support broader efforts to make water treatment technologies more accessible, affordable, and aligned with sustainability goals.

1.6 Thesis Outline

This thesis is organized into five chapters, each outlining a critical component of the research. Chapter 1 presents the research background, highlighting the growing concern of water pollution and the potential of photocatalytic degradation as a sustainable solution. This chapter also introduces a novel green electrochemical synthesis approach, utilizing bio-waste extracts and DES. The problem statement, research objectives, scope, and significance of the study are then addressed to give an overview of this work.

Chapter 2 provides a comprehensive review of relevant literature. It covers the characteristics and environmental impact of 2,4-DCP, the target pollutant in this study, and discusses heterogeneous photocatalysis as a treatment method. The photocatalytic properties of ZnO, including its degradation mechanisms, are explored. Various synthesis methods for ZnO are reviewed, with a particular focus on electrochemical approaches. The chapter also examines the potential of bio-waste extracts and DES to enhance the sustainability and efficiency of ZnO synthesis.

Chapter 3 details the methodology employed in this work. It includes descriptions of the materials and chemicals used, procedures for preparing bio-waste extracts and synthesizing DES, the preparation of ZnO photocatalysts, and the characterization techniques applied. The photocatalytic degradation experiments are also explained in detail.

Chapter 4 presents the results and discussions, divided into five key sections. The first section discusses the effects of different plant-based extracts on ZnO synthesis, and the second section explores the impact of DES incorporation on the electrosynthesis

process. The third section evaluates the photocatalytic degradation of 2,4-DCP, followed by an analysis of the degradation pathway in the fourth section. The final section compares the photocatalytic performance of the synthesized ZnO with that reported in other studies.

Finally, Chapter 5 concludes the thesis by summarizing the main findings and proposing recommendations for future research directions.

CHAPTER 2

LITERATURE REVIEW

2.1 Chlorophenol Derivatives as an Emerging Organic Pollutant

Due to rapid urbanization, new chemicals are introduced daily. In several industries, such as food processing, paper and pulp, iron and steel production, textiles, petrochemicals, agrochemicals, and cosmetics, almost 80,000 organic synthetic compounds are used extensively (Geetha & Nagarajan, 2021). The production, usage, and frequent release of organic pollutants have escalated into a serious global issue. These compounds, known for their acute and long-term harmful impacts on all living organisms, pose significant risks due to their tendencies for bioaccumulation and biomagnification. Such characteristics not only amplify the burden on ecosystems but also increase potential threats to human health. Common pollutants include industrial dyes, heavy metals, pharmaceuticals, and agricultural chemicals, especially chlorinated compounds like chlorophenols (CPs) and their derivatives.

2.1.1 Properties and Sources

CPs, which are the chlorinated aromatic compounds, are characterized by a structure comprising a benzene ring, an OH group, and chlorine atoms (Figure 2.1). Typically, CP compounds exist in solid form at room temperature, except for 2-CP, which remains in a liquid state. Their melting points range from 33 °C to 191 °C, and they generally exhibit limited solubility in water. The acidity of CPs is directly proportional to the number of chlorine atoms present, meaning that higher substitution of chlorine leads to increased acidity. Additionally, chlorination enhances the bioconcentration capability of CPs and their tendency to partition into sediments and lipids (Yadav et al., 2023).

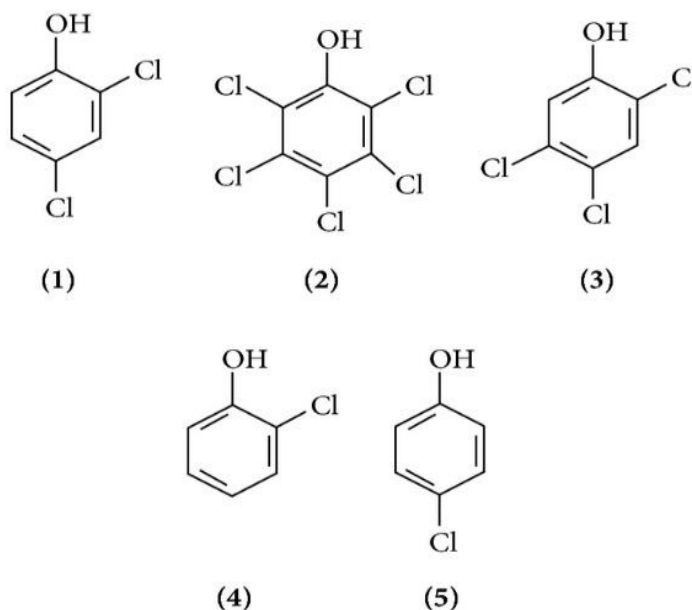


Figure 2.1 Chemical structures of the most common commercial chlorophenols:

(1) 2,4-dichlorophenol (2,4-DCP), (2) pentachlorophenol (PCP), (3) 2,4,5-trichlorophenol (2,4,5-TCP), (4) 2-chlorophenol (2-CP), and (5) 4-chlorophenol (4-CP)

The prevalence of CPs in the environment is a result of several factors, including industrialization, complex chemical processes, and shortcomings in treatment efficiency. Notably, CPs primarily originate from industrial waste and landfill leaching, while non-point sources encompass CP-based pesticides, chlorination in wastewater treatment, wood distillation processes, and storage tanks (Garba et al., 2019). Once released into the atmosphere, CPs can disperse over long distances via air currents before settling. Vapor emissions from CP production and the combustion of various substances such as municipal waste, hazardous waste, organic matter, coal, or wood contribute significantly to CP dispersal in the ambient air.

Although many CPs are not highly volatile and are released primarily through volatilization, compounds like trichlorophenols (TCP) and tetrachlorophenols (TeCPs),

which are marginally volatile, are predominantly emitted in vapor form. TCPs, for instance, have been detected in flue gas condensates from municipal incinerators, while DCPs, TCPs, and TeCPs have been found in emissions from oil and coal-fired power plants (Hamad et al., 2010).

Whereas, the presence of CPs in soil can originate from the accidental spills and the biodegradation of pesticides and herbicides, which often generate CPs as intermediate metabolites during the decomposition stage (Eslami et al., 2018). The other identified source includes the composting yards and municipal solid waste facilities (Yadav et al., 2023). Whereas, for PCPs, soil emission was evidenced due to PCP-based preservatives wood burning activity. Commonly, the organic content, porosity, water solubility, and biological processes controls the movement of CP contaminants in soil.

2.1.2 Exocological and Human Impacts

Toxicity refers to a chemical substance's ability to hurt biological systems. It is often associated with the level of exposure, chemical dose, exposure period, and biological system features. Given the high toxicity of CPs and their ubiquity in several environmental components, the effects on exposed species in soil, water, and vegetation have been elucidated in the previous literature.

In aquatic environments, the presence of CP derivatives especially, 2,4-DCP has been demonstrated to induce cellular and ecological toxicity in aquatic biosystems. A study on the genotoxic risks of 2,4-DCP on goldfish (*Carassius auratus*) found that 2,4-DCP compounds can significantly cause double-strand breaks (DNA damage) in goldfish species (Huang et al., 2018). When present in soil, the CPs have been linked with a severe threat to plants. Several studies highlighted the reduction in root length and seed germination in the soil-contaminated CPs (Ranjan et al., 2021). Other studies

on the effect of CP compounds on an algae species concluded that even at a low concentration of PCP (as low as 1 µg/L) can already cause serious growth inhibition (Yadav et al., 2023). It has also been known that the distribution of CPs in fish can exert the risks of serious disruption in free radical metabolism, immune factor response, apoptosis, and normal thyroid and gonad function which consequent in organs and endocrine systems failure, leads to uneven growth, deformity, and decreased reproductive rates (Ge et al., 2017).

In the meanwhile, the human exposure to CP has been linked to companies producing textiles, leather products, home preservatives, and petrochemicals. Occupational risks to this chemical have been observed to occur by inhalation and skin contact at work. Besides, workers' exposure has been documented at companies producing chlorinated pesticides or fungicides, as well as in industrial incinerators, waste treatment plants, and electrical utility linemen who come into touch with chlorophenol-treated poles used in electric line building (Zhang et al., 2023). Several health risks that have been reported due to these exposures include lymphoma, myocardial ischemia, and respiratory system-related diseases. Previously, a study remarked the positive correlation between non-Hodgkin's lymphoma occurrence in children and the pesticide application frequency.

Meanwhile, a study on 10,000 workers in vinyl chloride production factories found the workers mostly suffered from liver and lung cancer (Igbinosa et al., 2013). Additionally, more prior evidence of CP toxicity was described by Bukowska and coworkers who discovered various harmful effects of CPs in human erythrocytes (Bukowska et al., 2008). They discovered that CPs oxidize lipids and proteins resulting in the generation of reactive oxygen species (ROS) and a modification in the

antioxidative system (decreased glutathione levels and activity of catalase and superoxidative dismutase). Finally, chlorophenols altered the shape of erythrocytes (forming echinocytes) and caused hemolysis in these cells.

2.1.3 The Removal Technology

Due to ecotoxicity and health risks associated with the CPs, several eradication methods have been established which can be divided into two, biotic and abiotic methods. Biotic methods involve the utilization of bacteria and fungi as the degradation agent while the abiotic approaches mostly employ chemical techniques such as adsorption, membrane technology, photocatalysis, etc. The efforts in developing efficient degradation methods for the CPs degradation arise due to the complexity of CP degradation under the natural ambient (Yadav et al., 2023). This scenario is attributed to the stability of the aromatic ring in CP compounds and also the dependency on the degradability of CP itself under environmental variables such as the pH of the soil, water, or sediment.

Adsorption as one of the CP compound removal technologies has been acknowledged for its simplicity advantages, both in applicability and design. Diverse materials have been applied as adsorbents e.g., activated carbons, nanomaterials, agricultural wastes, biosorbents, and inorganic materials (Matei et al., 2022; Olu-Owolabi et al., 2017). Each material showed different adsorption capacity for the different CP compounds. For 2,4-DCP specifically, the adsorbents polyamide-based carbon nanofibers were found to be one of the efficient materials for the removal process. Meanwhile, for 4-CP, mesoporous carbon has been observed with the most absorptivity compared to nanocarbons, nanoporous graphene, and carbon nanofibers. For 2-CP, zeolite showed remarkable efficiency. Based on the reported findings,

typically the surface characteristic factors of the adsorbents especially the functional group, active sites, and surface charge determine the capacity of the adsorption. Other factors such as the reaction temperature as well as pH also play significant roles in influencing the performance of the adsorbents.

Other than that, membrane technology that encompasses ultra-filtration to micro-filtration is also one of the prominent CPs elimination strategies based on cost-efficiency, eco-friendliness, and scalability. Several membranes that have been proven to efficiently isolate CPs are polyamide-based i.e., NF-97, NF-99, and RO98 pHt membranes (Sewerin et al., 2021). However, it was highlighted that the removal percentage was highly affected by the initial concentration of the CP and also pressure. The higher pressure was enough to remove a lower concentration of CP from wastewater but not the case for wastewater with much concentrated CP. Hence, other removal technologies such as advanced oxidation processes or adsorption are required to support the membrane separation process (Saleh et al., 2020).

The limitations of the available wastewater treatments justified the development of novel technology such as the advanced oxidation process (AOP). This technique is credited with “the 21st century’s effluent treatment process” due to the ability of this technology to remove pollutants much more effectively than the present conventional treatment methods (Verma & Haritash, 2020). Unlike membrane technology and adsorption, which primarily function to separate CP compounds, AOP employing semiconducting materials can facilitate the degradation of these pollutants. The non-selectivity of AOP also allows almost every aqueous pollutant to be degraded through this route. Given the distinct benefit of treating effluent more rapidly and releasing fewer harmful intermediates, the method is beneficial in drastically reducing toxicity

levels and increasing the decomposition of contaminants, bringing them under permissible limits or below what conventional treatments fail to achieve. Mineralization is a mechanism by which contaminated materials are converted into non-toxic and stable inorganic substances like water, carbon dioxide, and salts (Hernández et al., 2022).. As a result, this constitutes a step advance in the degradation and treatment of toxicants that conventional approaches are unable to address due to their great resistance to degradation (Ong et al., 2018). The technique takes advantage of the strong reactive oxygen species ability to degrade a wide range of contaminants, including endocrine-disrupting chemicals (EDCs), persistent organic pollutants (POPs), total organic carbon (TOC), micropollutants, and even highly complex pharmaceutical waste containing antibiotics such as Amoxicillin (Verma & Haritash, 2020).

Another degradation pathway for CP compounds is via microbial degradation (using bacteria). Various studies using different cultures and strains of bacteria under aerobic and anaerobic conditions have been carried out. The best-described bacterium that degrades CP under anaerobic conditions is *Desulfomonile tiedjei*, a purely anaerobic Gram-negative sulfate-reducing bacterium, while the aerobic degradation of CPs by microorganisms requires enzymes such as oxygenases which incorporate atmospheric oxygen into their substrates (Nguyen & Khanal, 2018). However, the limitation of this route is regarding the deactivation problem of the bacteria due to their sensitivity towards pH levels in the feed and other substances in the wastewater. Due to the inconsistency of the temperature and seasonal variabilities of the natural environment, the promising degradation capacity achieved in real application is not as usually as successful as the laboratory scale (Yadav et al., 2023).

2.2 Types of AOP Mechanism for Pollutant Degradation

The fundamental of the AOP technique is the generation of powerful chemical oxidants in situ using ozone (O_3), hydrogen peroxide (H_2O_2), Fenton's reagent, UV light, or a catalyst. The hydroxyl radicals ($\cdot OH$) produced are powerful oxidizers capable of breaking down even the most resistant organic molecules (Ong et al., 2018). In detail, there are two types of AOP mechanisms: homogeneous and heterogeneous photocatalysis. Homogeneous photocatalysis uses Fenton's reagent, a combination of H_2O_2 and a Fe^{2+} salt, to generate H_2O_2 under UV irradiation at wavelengths above 300 nm. In contrast, heterogeneous photocatalysis uses semiconductor oxides as a photocatalyst (Anandan et al., 2020).

Previously, the photo-Fenton technique has been widely employed as a photo-AOP to eliminate organic contaminants from wastewater (Koltsakidou et al., 2019). This method is particularly suitable for sunlight-driven AOP because soluble iron-hydroxy and iron-organic acid complexes can absorb both ultraviolet and visible light. To avoid iron precipitation, the process operates at a pH level of approximately 3. However, achieving near-neutral pH conditions in wastewater treatment poses a significant challenge for the homogeneous photo-Fenton process, leading to increased operational costs associated with acidification and basification. Additionally, the iron sludge produced during the reaction must be removed (Mirzaei et al., 2016; Perini et al., 2018). The homogeneous Fenton process requires high concentrations of Fe^{n+} ions ($50-80 \text{ mg L}^{-1}$), which can result in significant environmental presence despite sludge precipitation. Moreover, ions present in wastewater can significantly influence the photo-Fenton process. Certain ions, such as halogens and sulfate, can form complexes with the catalyst, impacting its activity and favoring the formation of less reactive

radicals compared to H_2O_2 , depending on their concentrations and the pH of the solution. Therefore, understanding the role of ions in wastewater is crucial, given that their concentrations can vary from negligible to hundreds of grams (O'Dowd & Pillai, 2020).

After years of research, heterogeneous photocatalysis has emerged as a more advanced form of AOP, garnering continuous research attention. With semiconductor materials as photocatalysts, the degradation of pollutants can be accelerated. Activated by light energy, heterogeneous photocatalysts can generate highly reactive species such as superoxide ions ($\text{O}_2^{\cdot-}$), hydroxyl radical ($\cdot\text{OH}$), photogenerated holes (h^+), and peroxide radicals (HO_2^{\cdot}), capable of oxidizing a wide range of contaminant compounds and achieving total mineralization.

Various semiconductor materials have been investigated to ensure the efficiency of the pollutant degradation process. Especially, the metal oxides such as titanium dioxide (TiO_2), zinc oxide (ZnO), iron (III) oxide (Fe_2O_3), bismuth vanadium oxide (BiVO_4), copper oxide (CuO), silver oxide (Ag_2O), etc (Gao et al., 2013; Jing et al., 2022; A. Verma et al., 2019; Wu et al., 2019). The degradation application of various compounds including nitrogen-containing compounds, saturated hydrocarbons (alkanes), aromatic hydrocarbons, non-biodegradable azo dyes, volatile organic compounds, and pesticides using metal oxide-based semiconductors have been widely reported in the previous literature (Jing et al., 2022; Klu et al., 2022).

2.3 ZnO Semiconductor Photocatalyst

After TiO_2 , the reputation of ZnO as one of the photoactive semiconductors has been attributed to its well-known attractive prerequisites which are eco-friendliness and abundance making its application (for wastewater treatment) compatible with living

things and not posing any unfavorable risks to human or environmental health. ZnO is not only a superior semiconductor oxide with advantageous photophysical characteristics, but it also exhibits antibacterial qualities and can be produced at a significantly lower cost than TiO₂ photocatalysts (Sportelli et al., 2020; Uma et al., 2021).

2.3.1 Properties of ZnO

Having a standard band gap of 3.4 eV and a high exciton binding energy of 60 meV, ZnO is indeed a unique semiconductor. The fact that ZnO has the highest ionization energy for oxygen among all elements in the periodic table's sixth group confirms several of its unique properties (Sharma et al., 2022). ZnO is also employed as an ingredient in a growing range of industrial items, including paint, rubber, cosmetics, and coatings. ZnO nanostructures are also useful for solar cells and liquid crystal displays (Wibowo et al., 2020). Because of the lack of a center of symmetry in ZnO's wurtzite structure, there are significant electromechanical coupling effects in piezoelectric and pyroelectric properties, which can be used in piezoelectric sensors and mechanical actuators (Bhadwal et al., 2023; Guo, 2017).

Given its unique features, ZnO has received a lot of attention, particularly in the form of hexagonal wurtzite structures. Other structural forms of ZnO include cubic rocksalt and blende form. At moderate temperatures and pressures, it exhibits the thermodynamically stable wurtzite structure shown in Figure 2.2. At high pressures, ZnO becomes a cubic structure, making it an indirect band gap semiconductor ($E_g = 2.7$ eV) (Baranov et al., 2022). ZnO's hexagonal lattice is described as P6₃mc or C4_{6v}, with lattice constants "a = b = 0.32539 nm" and "c = 0.52098 nm" in a ratio of 1.6333.

Figure 2.2 shown the lattice structure of the ZnO 's wurtzite structure (Sharma et al., 2022).

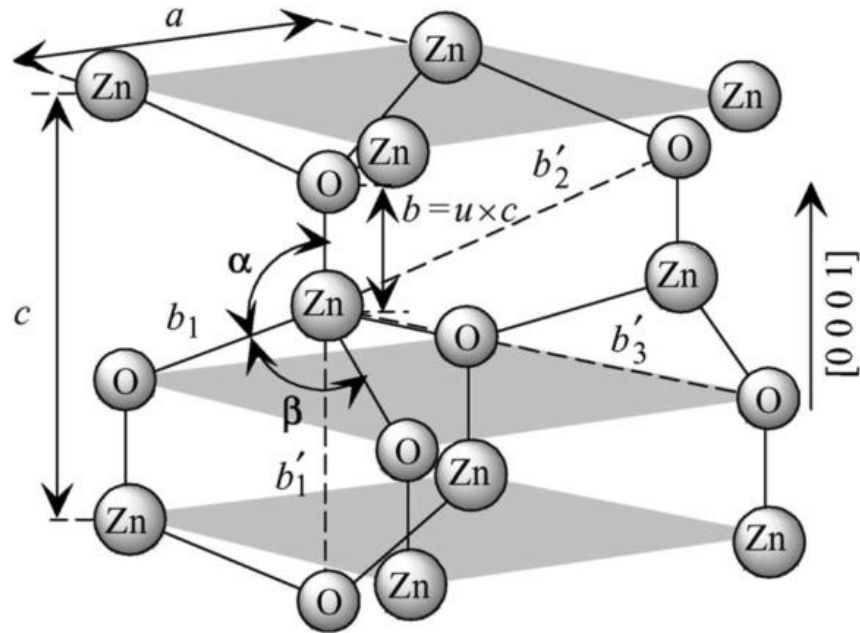


Figure 2.2 The illustrated ZnO's wurtzite structure (Sharma et al., 2022)

Each O^{2-} anion in the tetrahedron is bordered by four Zn^{2+} cations in the hexagonal structure of ZnO crystallizes. The wurtzite structure is made up of two interconnected hexagonal close-packed (hcp) sublattices of cation (Zn^{2+}) and anion (O^{2-}), each of which has one kind of atom displaced to the threefold c-axis. The basal plane and polar surface are two more important properties of ZnO. In addition, there is a steady polar plane $[0001]$, two non-polar surfaces $[10\bar{1}0]$ and $[11\bar{2}0]$, and one polar $[000\bar{1}]$. Facets exist in the structure of ZnO (Mohammad & Umar, 2010). Table 2.1 shows the basic physical properties of the ZnO structure.

Table 2.1 The ZnO basic physical parameters

Physical Parameters	Description
Stable phase at 300 K	Wurtzite
Lattice Constants	a = b = 0.32495 nm and c = 0.52069 nm
Melting points	1975 °C
Density	5.66 g/cm ³
Refractive index	2.01
Band gap	3.4 eV, Direct
Electron effective mass	0.24
Hole effective mass	0.59
Exciton binding energy	60 meV
Static dielectric constant	8.656

2.3.2 General Mechanism of ZnO in Pollutant Degradation

Mostly, the mechanism of ZnO photocatalysis during organic pollutant degradation can be summarized stepwise as follows:

- 1) The organic pollutants' diffusion onto the ZnO's surface
- 2) The organic pollutants' adsorption on the ZnO's surface
- 3) Redox reactions in the adsorbed phase
- 4) Desorption of products
- 5) Products eliminated from the region of the interface

When ZnO is exposed to solar light with photonic energy ($h\nu$) equal to or greater than the band gap energy (3.37 eV), electron (e^-) from the occupied valence band (VB) is excited to an empty conduction band (CB) (Ong et al., 2018). This light-triggered process produces e^-h^+ pairs (Figure 2.3). The e^-h^+ pairs can then migrate to the ZnO

surface and engage in redox processes, such as H^+ reacting with H_2O and OH^- ions to generate the $\cdot OH$ (Majumder et al., 2020). Meanwhile, $O_2^{\cdot -}$ anions are formed by the interaction of e^- with O_2 , which eventually yields H_2O_2 . The ensuing interaction between H_2O_2 and $O_2^{\cdot -}$ produces $\cdot OH$, a potent oxidizing agent that attacks contaminants on the ZnO surface, creating intermediates that will eventually change into green chemicals (Vora et al., 2009). The entire oxidation and reduction mechanism triggered by ZnO photocatalyst is shown in the equations below Eq. [2.1- 2.4].

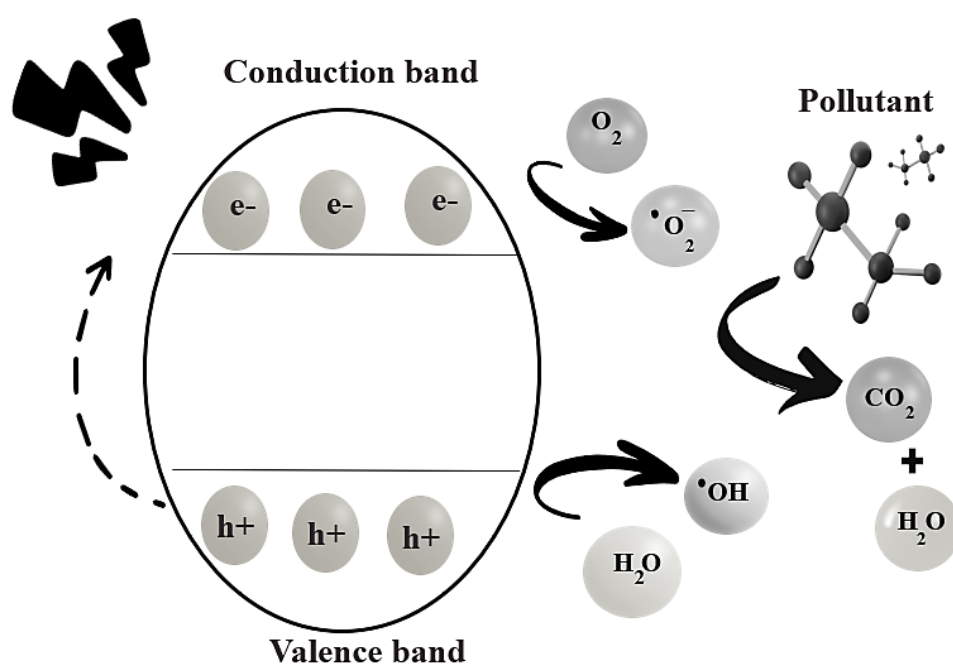


Figure 2.3 The photocatalytic mechanism by ZnO

